Supplement of Atmos. Chem. Phys., 16, 11125–11143, 2016
http://www.atmos-chem-phys.net/16/11125/2016/
doi:10.5194/acp-16-11125-2016-supplement

Atmospheric Chemistry and Physics
Open Access

Supplement of

Emission-dominated gas exchange of elemental mercury vapor over natural surfaces in China

Xun Wang et al.

Correspondence to: Xinbin Feng (fengxinbin@vip.skleg.cn) and Che-Jen Lin (jerry.lin@lamar.edu)

S1 An unpublished Hg concentration dataset

An unpublished Hg concentration dataset was collected in China in autumn of 2013 and 2014. This dataset includes Hg concentration in litterfall collected under 5 predominant tree species in 4 national subtropical evergreen forests (Xishuangbanna: 21.68 N, 101.42 E; Jianfengling: 19.18 N, 109.73 E; Shenlongjia: 31.45 N, 109.91 E; Mt. Wuyi: 28. 04 N, 117.57 E) and 4 national temperate forests (Jixian: 36.16 N, 110.73E; Mt. Xiaolong: 34.35 N, 106.01 E; Mt. Xiaoxinganling: 47.17 N, 128.95 E; Mt. Taihang: 34.96 N, 112.4 E). The collection of litter samples, measurement of Hg concentration and the quality control procedure have been described elsewhere (Zhou et al., 2013). Briefly, litterfall samples were collected by 1 m × 1 m nylon nets (1 mm pore size) placed under canopy. Hg concentration in litter was measured by a Lumex RA-915+ multifunctional Hg analyzer equipped with a pyrolysis attachment.

S2 Monte Carlo simulation for Hg input through litterfall in China

Monte Carlo simulation is a modeling technique that relies on random sampling and statistical data analysis (Raychaudhuri, 2008). In this study, Monte Carlo simulation was applied to integrate the datasets of Hg concentration in litterfall and litterfall biomass to produce the probabilistic Hg flux through litterfall, and described in detail in (Wang et al., 2016). Briefly, the simulation was carried out in three steps: creating statistical distribution using the observational data, perform random sampling, and flux calculation. In the first step, Hg concentration in litters and litterfall biomass production were regarded as random variables:

$$Hg_i(\theta) = f_\theta(x_1, x_2, \dots, x_n|\theta) \quad (1)$$

$$Biomass_i(\beta) = f_\beta(x_1, x_2, \dots, x_n|\beta) \quad (2)$$

where θ is a random variable vector for Hg concentrations in a given type of biomes group (total number of group is 14); β is the random variable vector for litterfall biomass production in i group (g m^{-2} yr^{-1}). Function f represents the associated probability density function. As such, F_θ and F_β represent the respective cumulative probability distribution functions.

After determining the respective probability density functions of the data, an inverse transformation method was utilized to generate a random sample from the probability density distribution (Raychaudhuri, 2008). For example, the random sample for Hg concentration (X) was generated using:

Generating: $U \sim U(0,1)$ (3)

Returning: $X = {F_\theta}^{-1}(U)$ (4)

where U is a uniform distribution and ${F_\theta}^{-1}$ denotes the inverse of F_θ. Similarly, the random sample for litterfall biomass production can be described as:

$$X_{\beta,i} \sim F_\beta(U)^{-1} \quad (5)$$

Therefore, the random variable of Hg deposition flux caused by litterfall (L_i) can be expressed as:

$$L_i = X_{\theta,i} X_{\beta,i} \quad (6)$$

After 50,000 sampling iterations, the descriptive statistics and the 95% confidence interval (CI) of L_i were calculated from the probability distribution of L_i. The Monte Carlo simulation and Hg flux calculation was performed using MATLAB 2013a and ArcGIS 10.3. The model-estimate Hg deposition (M_i, Mg yr^{-1}) was classified for the 14 WWF (World Wildlife Fund for Nature) biomes:

$$M_i = \frac{L_i}{t_{d,i}} \times t_{n,i} \times \sigma \quad (7)$$

Where L_i is Hg deposition flux caused by litterfall; σ is the ratio for unit conversion; $t_{d,i}$ is tree density (stems ha^{-1}); $t_{n,i}$ is total number of trees in the ith biomes type compiled from a best estimate in a recent study (Crowther et al., 2015) (http://elischolar.library.yale.edu/yale_fes_data/1). The global spatial distribution of Hg deposition through litterfall was then calculated based on the spatial distribution of tree density. The quality control procedure is described in detail by Wang et al. (2016).

Table S1 Orthogonal Design ($L_{25}(5^6)$) for WRF

Run Times	MP	CU	R	PBL
1	8	5	3	2
2	8	1	4	1
3	8	2	1	8
4	8	3	5	7
5	8	84	7	12
6	6	5	4	8
7	6	1	1	7
8	6	2	5	12
9	6	3	7	2
10	6	84	3	1
11	3	5	1	12
12	3	1	5	2
13	3	2	7	1
14	3	3	3	8
15	3	84	4	7
16	4	5	5	1
17	4	1	7	8
18	4	2	3	7
19	4	3	4	12
20	4	84	1	2
21	2	5	7	7
22	2	1	3	12
23	2	2	4	2
24	2	3	1	1
25	2	84	5	8

where MP: Microphysics Options, 8 means Thompson, 6 means WSM6, 3 means WSM3, 4 means WSM5, 2 means Lin scheme.

CU: Cumulus Parameterization Options； 1 means Kain-Fritsch; 2 means Betts-Miller-Janjic; 3 means Grell-Freitas; 5 means Grell-3; 84 means New SAS (HWRF).

R: Radiation Physics Options; 1 means Dudhia for ra_sw_physics and RRTM for ra_lw_physics ; 3 means CAM; 4 means RRTMG; 5 means New Goddard; 7 means FLG.

PBL: PBL Physics Options; 1 means YSU; 2 means MYJ; 7 means ACM2; 8 means BouLac; 12 means GBM.

Table S2 peer-reviewed air-surfaces fluxes data. W means warm season (May-October), and C means cold season (November-April).

Term	Lon	Lat	Type	Flux (ng m^{-2} h^{-1})	Refencens
Paddy	106.471	26.556	W	27.4	(Wang et al., 2004)
Paddy	106.471	26.556	C	5.6	(Wang et al., 2004)
Agricultural land	102.115	29.648	C	-4.1	(Fu et al., 2008)
Agricultural land	102.115	29.648	W	19.2	(Fu et al., 2008)
Agricultural land	102.115	29.648	W	21.1	(Fu et al., 2008)
Agricultural land	102.115	29.648	C	-3.1	(Fu et al., 2008)
Agricultural land	102.088	29.680	W	2.9	(Fu et al., 2008)
Agricultural land	102.088	29.680	C	1.5	(Fu et al., 2008)
Agricultural land	102.088	29.680	W	2.1	(Fu et al., 2008)
Agricultural land	102.225	29.787	W	132	(Fu et al., 2008)
Agricultural land	102.168	29.607	W	24.5	(Fu et al., 2008)
Agricultural land	102.115	29.648	W	20.4	(Fu et al., 2008)
Agricultural land	112.47	23.014	C	32.1	(Fu et al., 2012)
Grassland	112.852	22.997	C	114	(Fu et al., 2012)
Agricultural land	113.082	22.534	C	23.8	(Fu et al., 2012)
Grassland	113.706	22.82	C	75.6	(Fu et al., 2012)
Grassland	114.457	23.116	C	24.4	(Fu et al., 2012)
Grassland	113.542	23.859	C	44.8	(Fu et al., 2012)
Agricultural land	113.569	24.703	C	18.2	(Fu et al., 2012)
Agricultural land	112.87	23.022	C	135	(Fu et al., 2012)
Agricultural land	112.422	23.13	C	14.2	(Fu et al., 2012)
Agricultural land	112.68	22.336	C	10.7	(Fu et al., 2012)
Agricultural land	112.924	21.874	C	2.7	(Fu et al., 2012)
Agricultural land	113.893	23.407	C	1.4	(Fu et al., 2012)
Agricultural land	113.639	24.712	C	22.8	(Fu et al., 2012)
wheat	116.600	36.950	W	61.2	(Sommar et al., 2013)
Agricultural land	29.921	106.370	W	31	(Zhu et al., 2011)
Agricultural land	29.921	106.370	W	15.1	(Zhu et al., 2011)
Paddy	106.370	29.921	W	20.6	(Zhu et al., 2013)
Paddy	106.437	29.757	W	4.63	(Zhu et al., 2013)
wheat	116.600	36.950	W	7.6	(Zhu et al., 2015)
wheat	116.600	36.950	C	2.2	(Zhu et al., 2015)
wheat	116.600	36.950	W	7.2	(Zhu et al., 2015)
wheat	116.600	36.950	C	5.3	(Zhu et al., 2015)
wheat	116.600	36.950	W	10.8	(Zhu et al., 2015)
wheat	116.600	36.950	C	9.3	(Zhu et al., 2015)

wheat	116.600	36.950	W	17.3	(Zhu et al., 2015)
Longtanzi reservoir	106.400	29.817	W	43.75	(Wang et al., 2006)
Jialing river	106.433	29.833	C	6.7	(Wang et al., 2006)
Hongfeng reservoir	106.471	26.556	W	6.5	(Feng et al., 2008)
Hongfeng reservoir	106.471	26.556	C	5.1	(Feng et al., 2008)
Hongfeng reservoir	106.471	26.556	C	1.8	(Feng et al., 2008)
Hongfeng reservoir	106.471	26.556	W	4.8	(Feng et al., 2008)
Hongfeng reservoir	106.471	26.556	W	4	(Feng et al., 2008)
Hongfeng reservoir	106.471	26.556	C	2.8	(Feng et al., 2008)
Hongfeng reservoir	106.471	26.556	C	2	(Feng et al., 2008)
Baihua Reservoir	106.531	26.689	C	3	(Feng et al., 2004)
Baihua Reservoir	106.531	26.689	W	6.39	(Feng et al., 2004)
Baihua Reservoir	106.531	26.689	W	7.43	(Feng et al., 2004)
Baihua Reservoir	106.531	26.689	W	6.62	(Feng et al., 2004)
Wujiang reservoir	106.785	27.312	W	20.1	(Fu et al., 2010)
Wujiang reservoir WJD-1	106.785	27.312	C	6.2	(Fu et al., 2010)
Wujiang reservoir	106.785	27.312	W	14.1	(Fu et al., 2010)
Wujiang reservoir WJD-2	106.785	27.312	C	4.7	(Fu et al., 2010)
Wujiang reservoir	106.785	27.312	W	9.9	(Fu et al., 2010)
Wujiang reservoir WJD-3	106.785	27.312	C	3.2	(Fu et al., 2010)
Wujiang reservoir	106.769	27.321	W	4.1	(Fu et al., 2010)
Wujiang reservoir SFY-1	106.769	27.321	C	1	(Fu et al., 2010)
Wujiang reservoir	106.769	27.321	W	1.5	(Fu et al., 2010)
Wujiang reservoir SFY-2	106.769	27.321	C	0.6	(Fu et al., 2010)
Wujiang reservoir	106.769	27.321	W	4.4	(Fu et al., 2010)

Wujiang reservoir SFY-3	106.769	27.321	C	1.3	(Fu et al., 2010)
Puding reservoir	105.791	26.274	W	2.2	(Fu et al., 2010)
Puding reservoir	105.791	26.274	C	0	(Fu et al., 2013b)
Puding reservoir	105.791	26.274	W	4.2	(Fu et al., 2013b)
Puding reservoir	105.791	26.274	C	0.2	(Fu et al., 2013b)
HJD-1	104.114	37.550	W	4.2	(Fu et al., 2013b)
HJD-3	104.114	37.550	W	4.2	(Fu et al., 2013b)
HJD-1	104.114	37.550	C	3.1	(Fu et al., 2013a)
HJD-2	104.114	37.550	C	2.7	(Fu et al., 2013a)
HJD-3	104.114	37.550	C	2.1	(Fu et al., 2013a)
YZD-1	105.792	26.648	W	4	(Fu et al., 2013a)
YZD-2	105.792	26.648	W	3.9	(Fu et al., 2013a)
YZD-3	105.792	26.648	W	4	(Fu et al., 2013a)
YZD-1	105.792	26.648	C	0.1	(Fu et al., 2013a)
YZD-2	105.792	26.648	C	0.4	(Fu et al., 2013a)
YZD-3	105.792	26.648	C	1	(Fu et al., 2013a)
DF Reservoir	106.180	26.859	W	3.6	(Fu et al., 2013a)
DF Reservoir	106.180	26.859	W	4.3	(Fu et al., 2013a)
DF Reservoir	106.180	26.859	W	3.3	(Fu et al., 2013a)
DF Reservoir	106.180	26.859	C	0.7	(Fu et al., 2013a)
DF Reservoir	106.180	26.859	C	0.9	(Fu et al., 2013a)
SFY Reservoir	106.769	27.321	C	3.7	(Fu et al., 2013a)
SFY Reservoir	106.769	27.321	C	2.3	(Fu et al., 2013a)
SFY Reservoir	106.769	27.321	W	4.3	(Fu et al., 2013a)
SFY Reservoir	106.769	27.321	C	1.3	(Fu et al., 2013a)
SFY Reservoir	106.769	27.321	C	1.2	(Fu et al., 2013a)
SFY Reservoir	106.769	27.321	C	1.3	(Fu et al., 2013a)
East China sea shore soil	121.898	31.054	C	3.2	Zhu et al., 2013AEa
East China sea shore soil	121.898	31.054	C	-1.4	Zhu et al., 2013AEa
Subtropical forest soil	23.178	112.544	C	6.6	(Fu et al., 2012)
Subtropical forest soil	102.020	29.703	W	6.6	(Fu et al., 2008)
Subtropical forest soil	102.143	29.420	W	5.7	(Fu et al., 2008)
Subtropical forest soil	102.111	29.628	W	9.3	(Fu et al., 2008)

Subtropical forest soil	102.063	29.603	W	7.7	(Fu et al., 2008)
Subtropical forest soil	102.030	29.588	W	0.5	(Fu et al., 2008)
Subtropical forest soil	101.930	29.583	W	2.9	(Fu et al., 2008)
Subtropical forest soil	106.656	29.609	C	0.3	(Du et al., 2014)
Subtropical forest soil	106.283	29.833	W	14.2	(Ma et al., 2013)
Subtropical forest soil	106.283	29.833	W	20.7	(Ma et al., 2013)
Simianshan forest soil	106.4333	28.583	W	7.7	(Wang et al., 2006)
Geleshan forest soil	106.417	29.567	W	3.4	(Wang et al., 2006)
Jinyunshan forest soil	106.367	29.933	W	8.4	(Wang et al., 2006)
Changbai forest	128.112	42.402	W	2.7	(Fu et al., 2015)
Forest soil	125.299	43.850	W	7.6	(Fang et al., 2003)
Forest soil	125.467	43.780	W	5.6	(Fang et al., 2003)
Forest soil	125.467	43.780	W	3.3	(Fang et al., 2003)
Grassland	102.115	29.648	C	-18.7	(Fu et al., 2008)
Grassland	102.115	29.648	C	3.1	(Fu et al., 2008)
Grassland	102.115	29.648	W	13.4	(Fu et al., 2008)
Grassland	102.115	29.648	W	12.3	(Fu et al., 2008)
Grassland	102.115	29.648	W	-1.7	(Fu et al., 2008)
Grassland	106.731	26.512	W	58.9	(Feng et al., 2005)
Grassland	106.734	26.576	W	15.4	(Feng et al., 2005)
Grassland	106.798	26.533	W	7.9	(Feng et al., 2005)
Grassland	106.798	26.533	C	2.4	(Feng et al., 2005)
Grassland	106.798	26.533	W	12.2	(Feng et al., 2005)

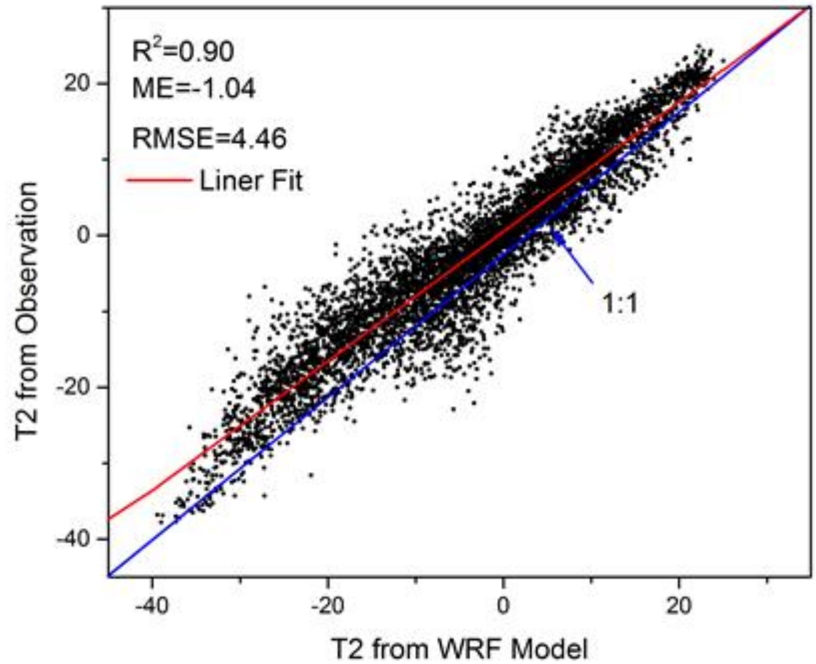

Figure S1 The simulated T2 (air temperature above 2 m) by WRF .vs the observed T2.

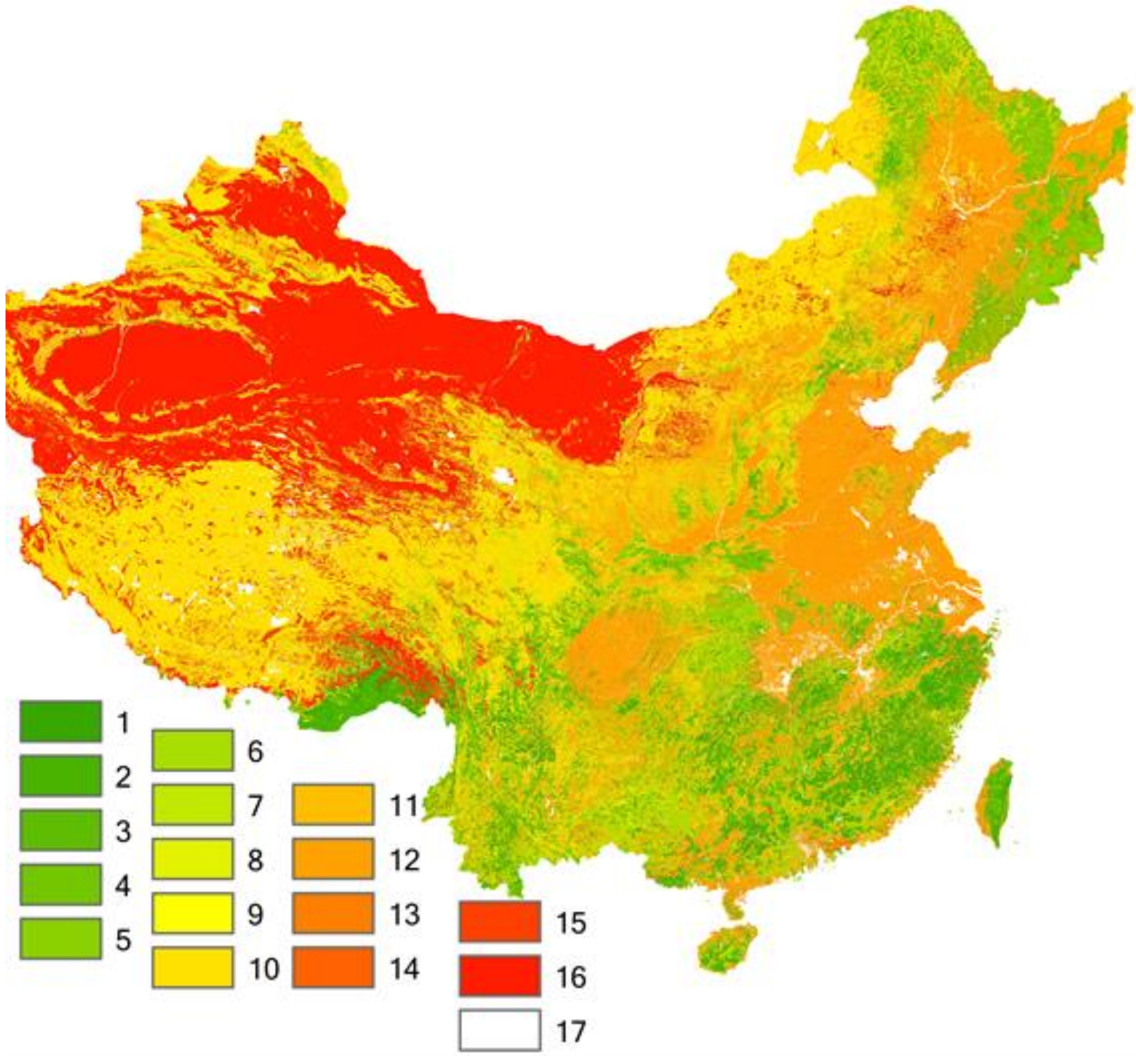

89

90 Figure S2 The spatial distribution of landuse in China. 1-17 means C1-C17.

91

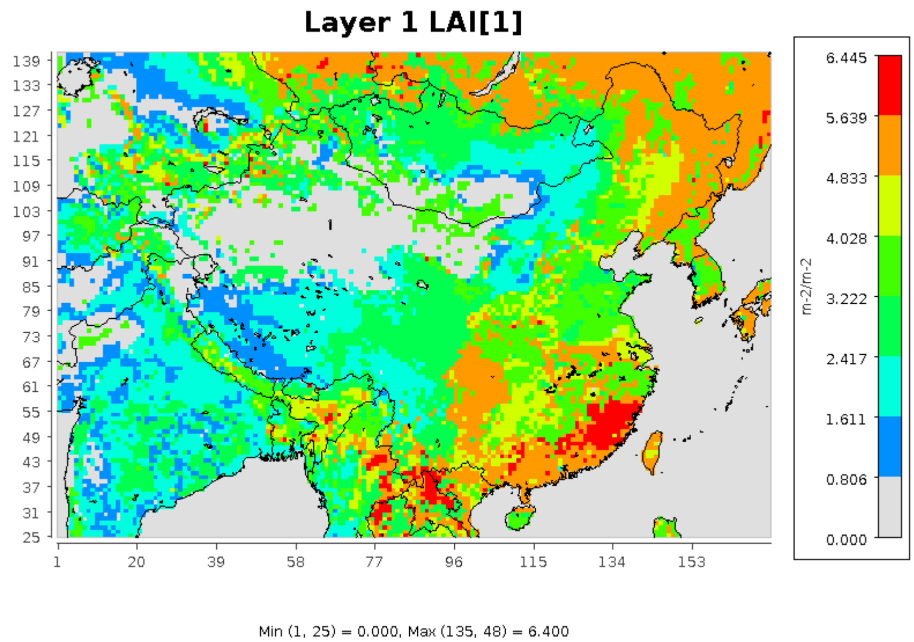

Figure S3 The spatial of mean LAI during summertime

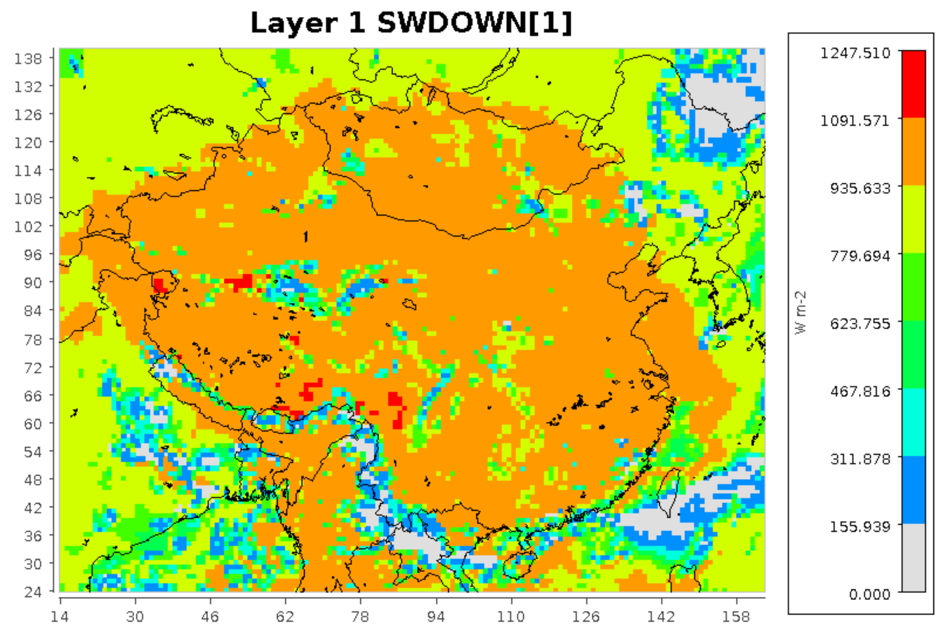

Figure S4 The spatial distribution of mean solar radiation at 14:00 during summertime.

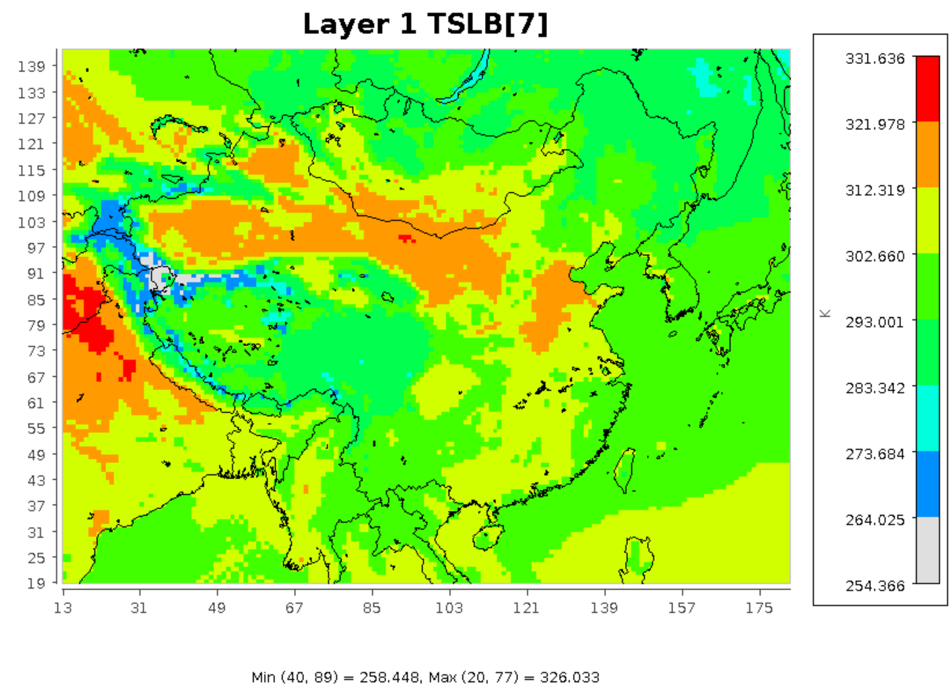

Figure S5 The spatial distribution of mean soil temperature at 14:00 during summertime.

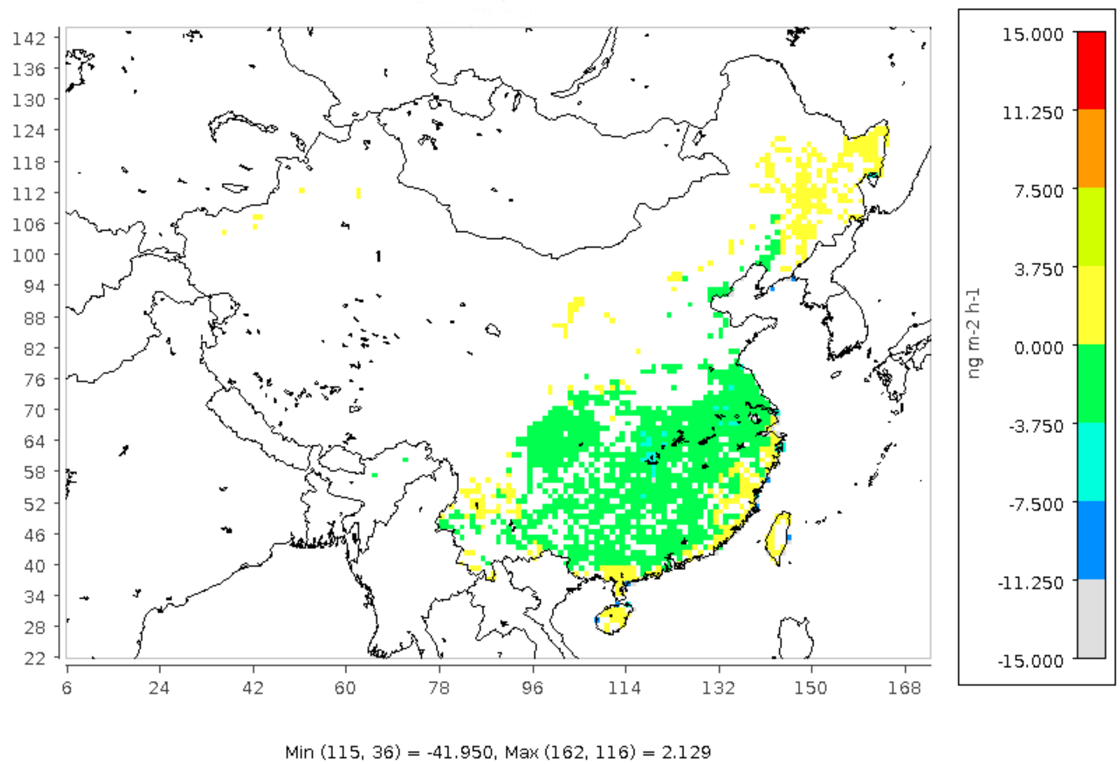

Figure S6. The simulated mean fluxes (ng m^{-2} h^{-1}) from rice paddy during Apr-Oct.

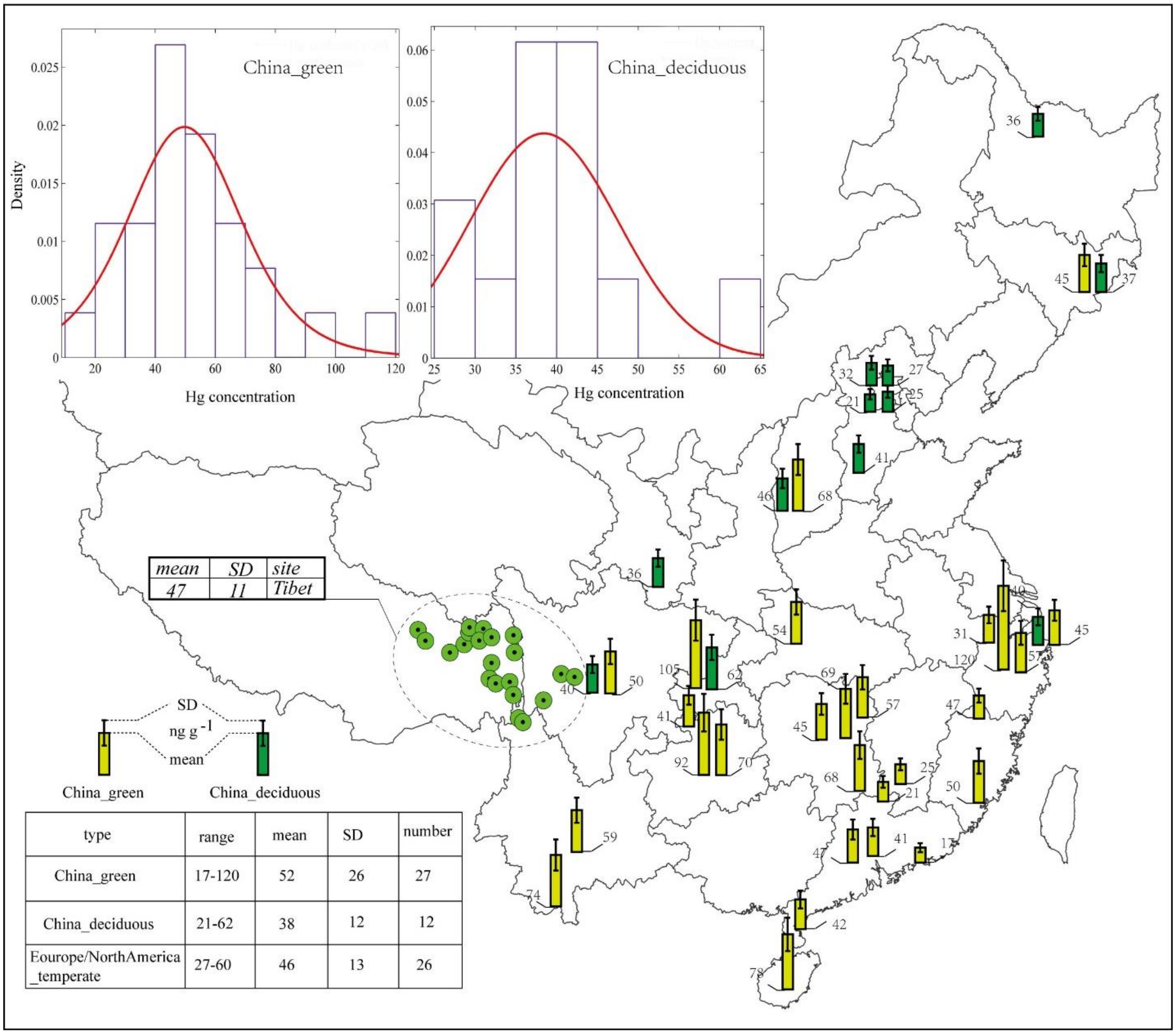

Figure S7. Database of Hg concentration in litterfall samples, China (Ma et al., 2015;Niu et al., 2011;Zhou et al., 2013;Fu et al., 2015;Wang et al., 2014;Tang et al., 2015;Juillerat et al., 2012;Blackwell et al., 2014;Risch et al., 2012;Selvendiran et al., 2008). An unpublished dataset including 8 sites in China is described in details in the SI. The Hg concentrations in evergreen and deciduous forests have a t Location-Scale distribution (μ=50.1, σ=19.3, F=6.6; and μ=36.3, σ=3.6, F=1.4, respectively).

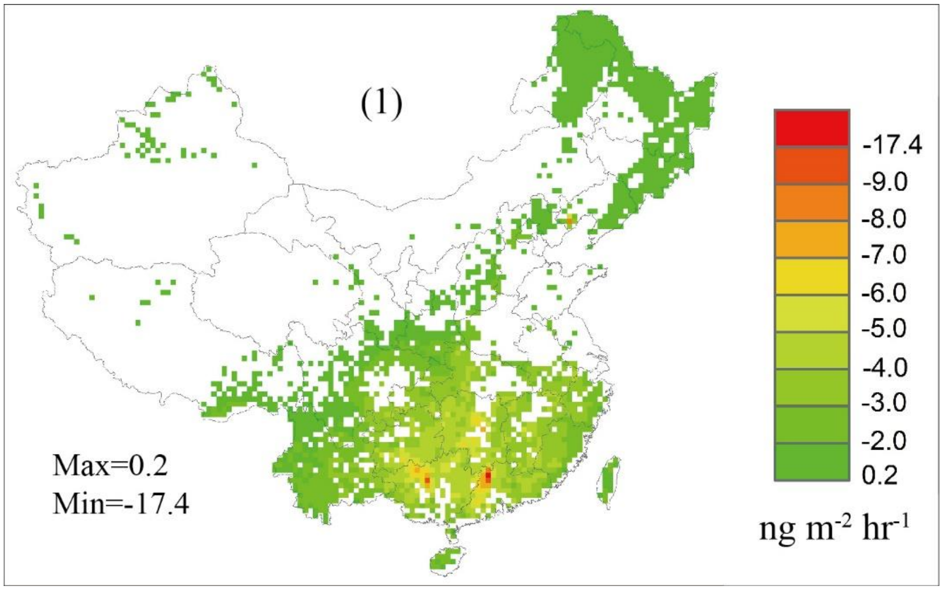

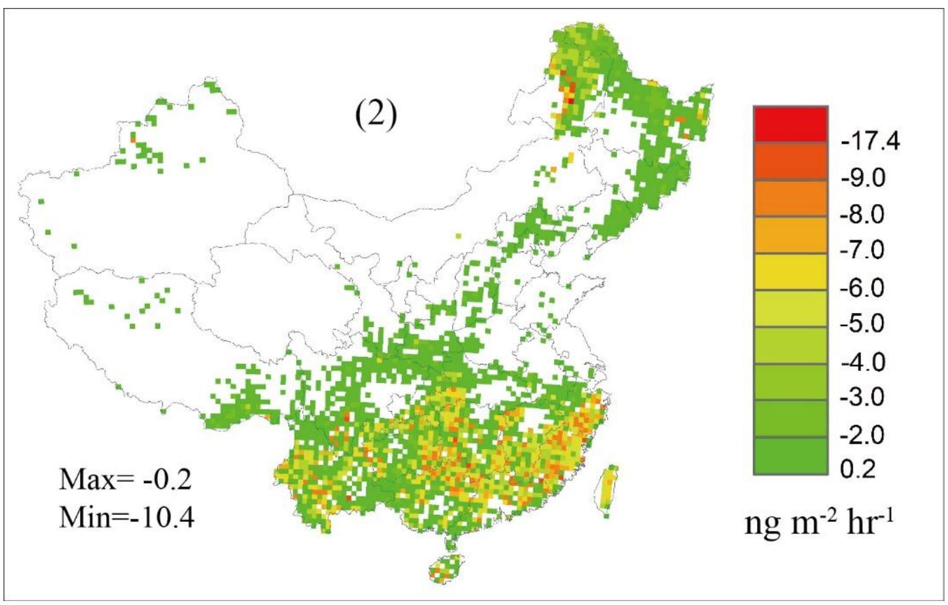

Figure S8. Comparison between: (1) the mean annual air-foliage flux in forest ecosystems predicted by the model developed in this study; (2) the observed Hg deposition through litterfall processed by Monte Carlo simulation (Wang et al., 2016). It is noted that the dataset size of (2) is about 5% large than the size of (1), because (2) contains trees in ecotone between forest and other landuses.

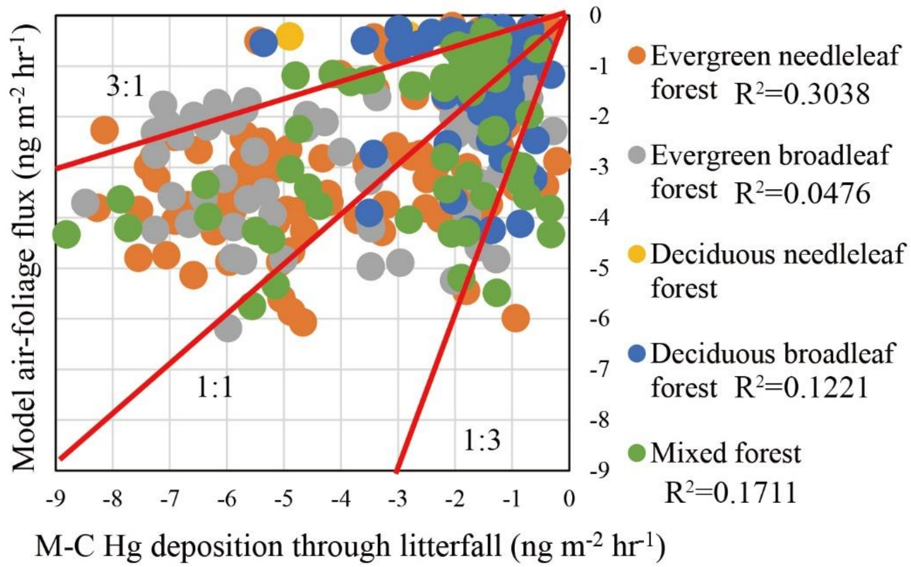

Figure S9. Scatterplot of observed Hg deposition through litterfall processed by Monte Carlo (M-C) simulation and the estimate air-foliage flux predicted by the model developed in this study.

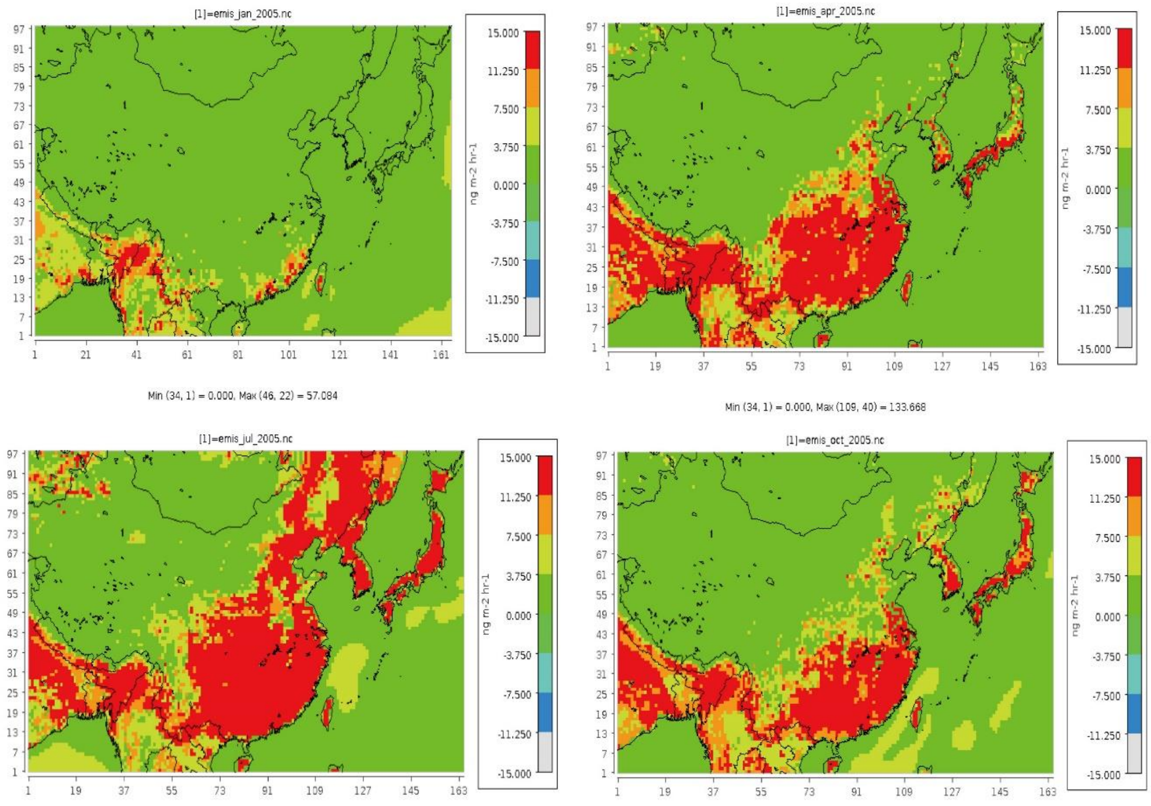

Figure S10. The simulated air-surfaces Hg^0 fluxes in East Asia (Shetty et al., 2008).

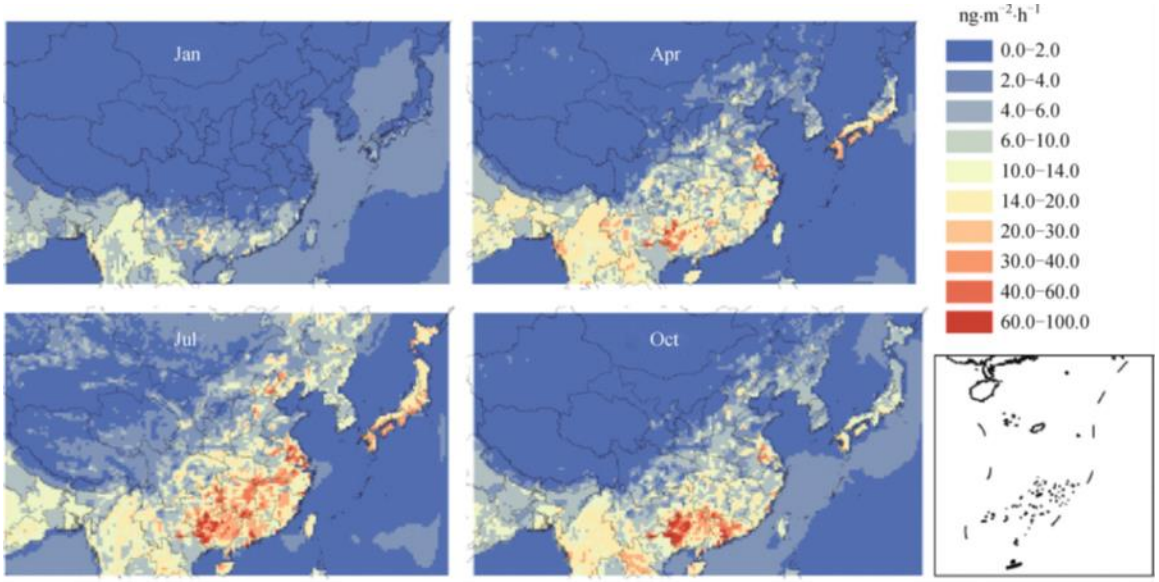

Figure S11. The simulated air-surfaces Hg^0 fluxes in East Asia (Wang et al., 2014).

References

Blackwell, B. D., Driscoll, C. T., Maxwell, J. A., and Holsen, T. M.: Changing climate alters inputs and pathways of mercury deposition to forested ecosystems, Biogeochemistry, 119, 215-228, 2014.

Crowther, T. W., Glick, H. B., Covey, K. R., Bettigole, C., Maynard, D. S., Thomas, S. M., Smith, J. R., Hintler, G., Duguid, M. C., Amatulli, G., Tuanmu, M. N., Jetz, W., Salas, C., Stam, C., Piotto, D., Tavani, R., Green, S., Bruce, G., Williams, S. J., Wiser, S. K., Huber, M. O., Hengeveld, G. M., Nabuurs, G. J., Tikhonova, E., Borchardt, P., Li, C. F., Powrie, L. W., Fischer, M., Hemp, A., Homeier, J., Cho, P., Vibrans, A. C., Umunay, P. M., Piao, S. L., Rowe, C. W., Ashton, M. S., Crane, P. R., and Bradford, M. A.: Mapping tree density at a global scale, Nature, 525, 201-205, 10.1038/nature14967 http://www.nature.com/nature/journal/v525/n7568/abs/nature14967.html#supplementary-information, 2015.

Du, B. Y., W, Q., Luo, Y., and Duan, L.: Field measurement of soil mercury emission in a Masson pine forest in Tieshanping, Chongqing in Southwestern China, Huan jing ke xue= Huanjing kexue / [bian ji, Zhongguo ke xue yuan huan jing ke xue wei yuan hui "Huan jing ke xue" bian ji wei yuan hui.], 35, 3830-3835, 2014.

Fang, F. M., Wang, Q. C., and Yin, J. H.: Mercury flux from urban soils and its potential factors (in Chinese), Sheng Tai Huan Jing, 3, 260-262, 2003.

Feng, X. B., Yan, H. Y., Wang, S. F., Qiu, G. L., Tang, S. L., Shang, L. H., Dai, Q. J., and Hou, Y. M.: Seasonal variation of gaseous mercury exchange rate between air and water surface over Baihua reservoir, Guizhou, China, Atmos Environ, 38, 4721-4732, 2004.

Feng, X. B., Wang, S. F., Qiu, G. A., Hou, Y. M., and Tang, S. L.: Total gaseous mercury emissions from soil in Guiyang, Guizhou, China, J Geophys Res-Atmos, 110, 2005.

Feng, X. B., Wang, S. F., Qiu, G. G., He, T. R., Li, G. H., Li, Z. G., and Shang, L. H.: Total gaseous mercury exchange between water and air during cloudy weather conditions over Hongfeng Reservoir, Guizhou, China, J Geophys Res-Atmos, 113, 2008.

Fu, X. W., Feng, X. B., and Wang, S. F.: Exchange fluxes of Hg between surfaces and atmosphere in the eastern flank of Mount Gongga, Sichuan province, southwestern China, Journal of Geophysical Research-Atmospheres, 113, 2008.

Fu, X. W., Feng, X. B., Wan, Q., Meng, B., Yan, H. Y., and Guo, Y. N.: Probing Hg evasion from surface waters of two Chinese hyper/meso-eutrophic reservoirs, Science of the Total Environment, 408, 5887-5896, 2010.

Fu, X. W., Feng, X. B., Zhang, H., Yu, B., and Chen, L. G.: Mercury emissions from natural surfaces highly impacted by human activities in Guangzhou province, South China, Atmos Environ, 54, 185-193, 2012.

Fu, X. W., Feng, X. B., Guo, Y. N., Meng, B., Yin, R. S., and Yao, H.: Distribution and production of reactive mercury and dissolved gaseous mercury in surface waters and water/air mercury flux in reservoirs on Wujiang River, Southwest China, J Geophys Res-Atmos, 118, 3905-3917, 2013a.

Fu, X. W., Feng, X. B., Yin, R. S., and Zhang, H.: Diurnal variations of total mercury, reactive mercury, and dissolved gaseous mercury concentrations and water/air mercury flux in warm and cold seasons from freshwaters of southwestern China, Environ Toxicol Chem, 32, 2256-2265, 2013b.

Fu, X. W., Zhang, H., Wang, X., Yu, B., Lin, C.-J., and Feng, X. B.: Observations of atmospheric mercury in China: a critical review, Atmos. Chem. Phys. Discuss., 11925-11983, doi:10.5194/acpd-15-11925-2015, 2015.

Juillerat, J. I., Ross, D. S., and Bank, M. S.: Mercury in litterfall and upper soil horizons in forested ecosystems in Vermont, USA, Environmental Toxicology and Chemistry, 31, 10.1002/etc.1896, 2012.

Ma, M., Wang, D. Y., Sun, R. G., Shen, Y. Y., and Huang, L. X.: Gaseous mercury emissions from subtropical forested and open field soils in a national nature reserve, southwest China, Atmos Environ, 64, 116-123, 2013.

Ma, M., Wang, D. Y., Du, h. X., Z, Z., and W, S. Q.: Atmospheric mercury deposition and its contribution of the regional atmospheric transport to mercury pollution at a national forest nature reserve, southwest China, Environ Sci Pollut R, DOI 10.1007/s11356-015-5152-9, 2015.

Niu, Z., Zhang, X., Wang, Z., and Ci, Z.: Mercury in leaf litter in typical suburban and urban broadleaf forests in China, J Environ Sci-China, 23, 2042-2048, 10.1016/s1001-0742(10)60669-9, 2011.

Raychaudhuri, S.: INTRODUCTION TO MONTE CARLO SIMULATION, Proceedings of the 2008 Winter Simulation Conference, 91-100, 2008.

Risch, M. R., DeWild, J. F., Krabbenhoft, D. P., Kolka, R. K., and Zhang, L. M.: Litterfall mercury dry deposition in the eastern USA, Environ Pollut, 161, 284-290, 2012.

Selvendiran, P., Driscoll, C. T., Montesdeoca, M. R., and Bushey, J. T.: Inputs, storage, and transport of total and methyl mercury in two temperate forest wetlands, J Geophys Res-Biogeo, 113, 2008.

Shetty, S. K., Lin, C. J., Streets, D. G., and Jang, C.: Model estimate of mercury emission from natural sources in East Asia, Atmos Environ, 42, 8674-8685, 2008.

Sommar, J., Zhu, W., Shang, L. H., Feng, X. B., and Lin, C. J.: A whole-air relaxed eddy accumulation measurement system for sampling vertical vapour exchange of elemental mercury, Tellus B, 65, 2013.

Tang, R., Wang, H., Luo, J., Sun, S., Gong, Y., She, J., Chen, Y., Dandan, Y., and Zhou, J.: Spatial distribution and temporal trends of mercury and arsenic in remote timberline coniferous forests, eastern of the Tibet Plateau, China, Environ Sci Pollut R, 22, 11658-11668, 10.1007/s11356-015-4441-7, 2015.

Wang, D. Y., He, L., Shi, X. J., Wei, S. Q., and Feng, X. B.: Release flux of mercury from different environmental surfaces in Chongqing, China, Chemosphere, 64, 1845-1854, 2006.

Wang, S., Zhang, L., Wang, L., Wu, Q., Wang, F., and Hao, J.: A review of atmospheric mercury emissions, pollution and control in China, Frontiers of Environmental Science & Engineering, 8, 631-649, 10.1007/s11783-014-0673-x, 2014.

Wang, S. F., Feng, X. B., Qiu, G. L., and Fu, X. W.: comparision of air/soil mercury exchange betwwen warm and cold season in Hongfeng reservior region, Huan jing ke xue= Huanjing kexue / [bian ji, Zhongguo ke xue yuan huan jing ke xue wei yuan hui "Huan jing ke xue" bian ji wei yuan hui.], 25, 123-127, 2004.

Wang, X., Bao, Z., Lin, C.-J., Yuan, W., and Feng, X.: Assessment of global mercury deposition through litterfall, Environ Sci Technol, 10.1021/acs.est.5b06351, 2016.

Zhou, J., Feng, X. B., Liu, H. Y., Zhang, H., Fu, X. W., Bao, Z. D., Wang, X., and Zhang, Y. P.: Examination of total mercury inputs by precipitation and litterfall in a remote upland forest of Southwestern China, Atmos Environ, 81, 364-372, 2013.

Zhu, J., Wang, D., Liu, X., and Zhang, Y.: Mercury fluxes from air/surface interfaces in paddy field and dry land, Applied Geochemistry, 26, 10.1016/j.apgeochem.2010.11.025, 2011.

Zhu, J. S., Wang, D. Y., and Ma, M.: Mercury release flux and its influencing factors at the air-water interface in paddy field in Chongqing, China, Chinese Sci Bull, 58, 266-274, 2013.

Zhu, W., Sommar, J., Lin, C. J., and Feng, X.: Mercury vapor air-surface exchange measured by collocated micrometeorological and enclosure methods - Part I: Data comparability and method characteristics, Atmos

Chem Phys, 15, 685-702, 2015.